Dissociation of diabetes and obesity in mice lacking orphan nuclear receptor small heterodimer partner[s]

Young Joo Park,[1,†,]* Seong Chul Kim,[§] Jeehee Kim,[§] Sayeepriyadarshini Anakk,* Jae Man Lee, * Hsiu-Ting Tseng,* Vijay Yechoor,** Junchol Park,[††] June-Seek Choi,[††] Hak Chul Jang,[†] Ki-Up Lee,[§§] Colleen M. Novak,*** David D. Moore,[2,]* and Yoon Kwang Lee[1,2,§,]*

Department of Molecular and Cellular Biology,* and Division of Diabetes, Endocrinology, and Metabolism and Department of Medicine,**Baylor College of Medicine, Houston, TX; Department of Internal Medicine,[†] Seoul National University Bundang Hospital, Seongnam, Korea; Department of Integrative Medical Sciences,[§] Northeast Ohio Medical University, Rootstown, OH; Department of Psychology,[††] Korea University, Seoul, Korea; Department of Internal Medicine,[§§] University of Ulsan College of Medicine, Seoul, Korea; and Department of Biological Sciences,*** Kent State University, Kent, OH

Abstract Mixed background $SHP^{-/-}$ mice are resistant to diet-induced obesity due to increased energy expenditure caused by enhanced PGC-1α expression in brown adipocytes. However, congenic $SHP^{-/-}$ mice on the C57BL/6 background showed normal expression of PGC-$1α$ and other genes involved in brown adipose tissue thermogenesis. Thus, we reinvestigated the impact of small heterodimer partner (SHP) deletion on diet-induced obesity and insulin resistance using congenic $SHP^{-/-}$ mice. Compared with their C57BL/6 wild-type counterparts, $SHP^{-/-}$ mice subjected to a 6 month challenge with a Western diet (WestD) were leaner but more glucose intolerant, showed hepatic insulin resistance despite decreased triglyceride accumulation and increased β-oxidation, exhibited alterations in peripheral tissue uptake of dietary lipids, maintained a higher respiratory quotient, which did not decrease even after WestD feeding, and displayed islet dysfunction. Hepatic mRNA expression analysis revealed that many genes expressed higher in $SHP^{-/-}$ mice fed WestD were direct peroxisome proliferator-activated receptor alpha (PPARα) targets. Indeed, transient transfection and chromatin immunoprecipitation verified that SHP strongly repressed PPARα-mediated transactivation.▮▮ SHP is a pivotal metabolic sensor controlling lipid homeostasis in response to an energy-laden diet through regulating PPARα-mediated transactivation. The resultant hepatic fatty acid oxidation enhancement and dietary fat redistribution protect the mice from diet-induced obesity and hepatic steatosis but accelerate development of type 2 diabetes.—Park, Y. J., S. C. Kim, J. Kim, S. Anakk, J. M. Lee, H-T. Tseng, V. Yechoor, J. Park, J-S. Choi, H. C. Jang, K-U. Lee, C. M. Novak, D. D. Moore, and Y. K. Lee. **Dissociation of diabetes and obesity in mice lacking orphan nuclear receptor small heterodimer partner.** *J. Lipid Res.* 2011. 52: 2234–2244.

A primary physiological function of the orphan nuclear receptor small heterodimer partner (SHP) is in the negative feedback regulation of $Cyp7A1$ gene expression in response to elevated bile acids (1, 2), although SHP independent bile acid feedback pathways have also been suggested (3–5). In addition, SHP plays a role in the basal bile flow rate through regulation of the bile salt export pump, BSEP (6).

Interaction of SHP with hepatocyte nuclear factor alpha (HNF4α), a gene responsible for maturity-onset diabetes of the young, suggested possible linkage between SHP and diabetes (7). Indeed, several heterozygous mutations in the SHP gene have been found in mildly obese Japanese subjects with maturity-onset diabetes of the young (8). Additional analysis revealed that the SHP mutations cosegregated with obesity but not with diabetes. Novel genetic variants were also found in UK and Danish populations,

Abbreviations: ACC1, acetyl-Coenzyme A carboxylase alpha; Acox, acyl-Coenzyme A oxidase; BAT, brown adipose tissue; CAV-1, caveolin 1; CD, chow diet; ChIP, chromatin immunoprecipitation; CPT-1a, carnitine palmitoyltransferase 1a; DIO, diet induced obesity; DIO2, deiodinase type 2; FATP, fatty acid transporter; GSIS, glucose-stimulated insulin secretion; GTT, glucose tolerance test; HMGCoAS, 3-hydroxy-3-methylglutaryl-Coenzyme A synthase; HSL, hormone sensitive lipase; ITT, insulin tolerance test; MCAD, medium chain acyl-Coenzyme A dehydrogenase; ME, malic enzyme; RQ, respiratory quotient; SCD-1, stearoyl-Coenzyme A desaturase 1; SHP, small heterodimer partner; SRBI, scavenger receptor class B, member 1; TG, triglyceride; UCP-1, uncoupling protein-1; WestD, Western diet; WT, wild type.

[1] These authors equally contributed to this work.
[2] To whom correspondence should be addressed.
  e-mail: ylee3@neomed.edu (Y.K.L.); moore@bcm.tmc.edu (D.D.M.)
[s] The online version of this article (available at http://www.jlr.org) contains supplementary data in the form of eight figures.

but only the variants in UK subjects were linked to obesity (9–11). Importantly, all key *SHP* variants were associated with loss of the HNF4α inhibition.

Development of type 2 diabetes is strongly associated with obesity and hepatic steatosis (12, 13). The adverse effect of liver fat accumulation on glucose homeostasis is one of several cornerstones of the metabolic syndrome. An earlier study with mixed background $SHP^{-/-}$ mice revealed that they were protected from diet-induced obesity (DIO) and showed improved glucose homeostasis and decreased hepatic steatosis (14). These phenotypes were attributed to increased whole-body energy expenditure by brown adipose tissue (BAT) where major genes involved in energy expenditure were upregulated. However, congenic C57BL/6 $SHP^{-/-}$ mice (6) fed the same Western diet (WestD) were also resistant to DIO, but the expression of these genes in BAT was not altered. Therefore, we reinvestigated the phenotype of DIO resistance in congenic $SHP^{-/-}$ mice and observed a distinctive series of metabolic signatures including whole-body glucose intolerance, inflexible RQ, and lipid redistribution. Many strongly upregulated genes in $SHP^{-/-}$ mice fed WestD are direct targets of PPARα and HNF4α. Thus, the loss of SHP results in a disruption of the association between fat accumulation and insulin sensitivity.

MATERIALS AND METHODS

Animals and treatments

The congenic $SHP^{-/-}$ mice used for this experiment were generated by backcrossing to C57BL/6 mice (Harlan, Indianapolis, IN) for 10 generations (6) and only male mice were used throughout experiments. Age-matched male C57BL/6 mice (Harlan) were bred and housed in the same room along with $SHP^{-/-}$ mice. The mice were fed a WestD [Harlan; 21% (w/w) total lipid (42% calories from fat), 0.2% (w/w) cholesterol, 4.5 kcal/g] or chow diet [CD; Test Diet, Richmond, IN, 5% (w/w) total lipid (13% calories from fat), <0.04% (w/w) cholesterol, 4.07 kcal/g] for 12–24 weeks as indicated. All tissues and blood were collected after overnight fasting. Glucose tolerance tests (GTT) were performed by intraperitoneal injection of glucose (1 g/kg for WestD-fed groups or 2 g/kg for Chow-fed groups) after overnight fasting. Insulin tolerance tests (ITT) were performed by intraperitoneal injection of 1 U/kg insulin (humulin; Lilly, Indianapolis, IN) 6 h after food removal. Blood glucose was measured on tail vein samples using One Touch glucometer (LifeScan, Milpitas, CA). Mice were maintained in the accredited pathogen-free facilities at Northeast Ohio Medical University, Baylor College of Medicine, or Seoul National University Bundang Hospital on a 12 h light/dark cycle and fed a standard rodent CD and water was available ad libitum. All animals received humane care according to the criteria outlined in the "Guide for the Care and Use of Laboratory Animals" prepared by the National Academy of Sciences and published by the National Institutes of Health (NIH publication 86-23, revised 1985) and all protocols for animal use were approved by these institutes.

Insulin sensitivity and Western blotting

Mice fed WestD for 22 weeks were injected with 5 U/kg of humulin after overnight fasting. Mice were euthanized 5 min after the injection and livers and quadriceps were collected. Twenty micrograms of proteins from the tissues were subjected to Western blot.

After probing with anti phospho-Akt (Ser473) or Akt antibodies (1:1000 dilution, Cell Signaling, Beverly, MA), the specific protein bands were visualized by a chemiluminescence system (Thermo Scientific, Rockford, IL) after incubation with HRP-linked secondary antibodies (1:5000 dilution, Invitrogen, Carlsbad, CA). The same membranes were stripped and reprobed with anti-β-actin antibody (1:1000 dilution, Santa Cruz, Santa Cruz, CA).

Indirect calorimetry and activity measurement

Oxymax system (Columbus Instruments, Columbus, OH) was used for indirect calorimetry at the Baylor mouse phenotyping core facility. All the parameters were measured every 10 min for 24 h and normalized to lean mass. Physical activity was measured in a separate group of mice (n = 6 per group) using infrared photocell-based activity monitor from Columbus Instruments at Kent State University. Beam breaks were recorded every 10 s for the duration of the 24 h study.

Transient transfection and ChIP

A luciferase reporter gene driven by three copies of the PPAR binding element from the Acox1 (acyl-CoA oxidase) promoter (15), actin-β-galactosidase (16), PPARα and/or retinoid X receptor (RXRα) expression plasmids were cotransfected into HepG2 cells along with cytomegalovirus promoter-driven CDM8 (17) or CDM8mSHP using Fugene reagent (Roche, Indianapolis, IN). After overnight culture, cells were replenished with media containing charcoal stripped serum plus DMSO, 2 nM GW7647 (PPARα-specific agonist, Cayman Chem, Ann Arbor, MI), 1 μM LG1069 (RXR-specific agonist, LC labs, Woburn, MA), or 10 μM 9-*cis* retinoic acid (Biomol, Farmingdale, NY) and incubated another 24 h before harvest for luciferase assy. Dual-light combined reporter gene assay system (Applied Biosystems, Carlsbad, CA) was used to measure luciferase and β-galactosidase activities. For chromatin immunoprecipitation (ChIP) assay, mouse liver nuclei were isolated and sonicated to solubilize chromosomal DNAs and their associated proteins after crosslinking with formaldehyde treatment. The extracts were incubated with anti-PPARα, anti-SHP antibodies, or IgG (Santa Cruz) overnight and the immunocomplexes were precipitated using protein A agarose (Millipore, Bedford, MA). After decrosslinking, immunoprecipitated DNA fragments were amplified by PCR using primers (forward: 5′-tagccaacgacaatgaacc-3′, reverse: 5′-cggaaaccagaagggaatg-3′) designed for mouse Acox1 promoter region containing two PPAR binding elements. As a negative control, primers designed for -7.5kb upstream of Acox1 start codon were used.

Serum and tissue chemistry

Unless otherwise indicated, blood was drawn from orbital plexus after overnight fasting and glucose was measured with One Touch glucometer. Serum was prepared in Terumo Capiject tube (Fisher, Pittsburgh, PA) and stored at −80°C until use. Lipids were extracted from liver using chloroform-methanol extraction (18). Enzymatic assay kits were used for the determination of non-esterified fatty acids (Wako, Richmond, VA), cholesterol, and triglyceride (TG) (Thermo Scientific). Hepatic lipids were normalized to the dried liver weight after chloroform-methanol extraction. Insulin concentration was measured using a mouse/rat insulin ELISA kit (Millipore). Hepatic glycogen content was determined using a commercial kit (Biovision, Mountain View, CA).

Quantitative real-time PCR

Quantitative PCR (qPCR, SYBR green or TaqMan) analysis was performed on an ABI prism 7500 sequence detection system (Applied Biosystems). Expression was normalized to GAPDH and the relative quantification was calculated using ΔCt values. The real-time PCR primer and probe sets were purchased from Qiagen

(SYBR green analysis) or Applied Biosystems (TaqMan analysis) except mouse SHP (forward: 5′- tgggtcccaaggagtatgc-3′, reverse: 5′- gctccaagacttcacacagtg-3′).

Determination of fatty acid oxidation and hepatic TG secretion

The fatty acid oxidation rate was evaluated by $^{14}CO_2$ generation from [^{14}C]palmitate (PerkinElmer, Waltham, MA) using mouse liver homogenates as previously described (19) with some modifications. An amount of 20–25 mg of liver samples was minced and homogenized in 500 µl of sucrose-EDTA buffer by thirty strokes with a Teflon pestle at 1,200 rpm. A total of 50 µl of the homogenates was mixed with 150 µl incubation buffer in a well adjacent to a well containing 200 µl 1M NaOH. After incubation for 2 h in a 30°C water bath with constant agitation, the reaction was terminated by addition of 50 µl 4N sulfuric acid. Radioactivity of CO_2 trapped in 150 µl NaOH solution was determined using liquid scintillation counter and normalized to protein concentration of the initial homogenates. To measure hepatic TG secretion, mice fed either CD or WestD (3 weeks) were injected intraperitoneally with 1,000 mg/kg of poloxamer 407 4 h after food removal as described (20). Serum TG content at each time point was determined by Infinity TG kit (Thermo Scientific).

Tissue distribution of dietary fat

To determine tissue distribution of dietary fat, 2-month-old mice were orally challenged with 200 µl olive oil containing 2µCi [^{14}C]trioleoylglycerol (PerkinElmer) after overnight fasting. Four hours later, mice were euthanized to collect liver, quadriceps, and epididymal fat for their radioactivity levels.

Islet isolation and insulin secretion in static incubation

Islets were isolated using pancreatic perfusion with collagenase solution (type XI, Sigma, St. Louis, MO) followed by Neutral Red staining. The stained islets were hand picked under a microscope. Ten similar sized islets were used for in vitro glucose-stimulated insulin secretion (GSIS) after overnight incubation in serum free RPMI media containing 11.1 mM glucose. Media were collected 30 min after glucose challenge. Insulin contents of the islets were measured after acid ethanol lysis and normalized to protein concentration.

Statistics

Data were presented as means ± SEM. All the p-values, if not specified, were obtained using 2-way ANOVA with Bonferroni posttests.

RESULTS

$SHP^{-/-}$ mice are resistant to WestD-induced obesity with normal brown adipocyte function

On a control CD, young adult congenic $SHP^{-/-}$ mice showed no difference in body weight gain compared with WT mice. However, at 70 weeks, they weighed approximately 10% less than age-matched WT mice (**Fig. 1A**). When WT and $SHP^{-/-}$ mice were fed WestD, a body weight difference was evident as early as 2 weeks, similar to the previous study with mixed background $SHP^{-/-}$ mice (Fig. 1B). Analysis of body composition using dual energy X-ray absorptiometry revealed a dramatic difference in fat mass between WestD-fed WT and $SHP^{-/-}$ mice (**Table 1**).

Contrary to previous results, however, expression of major energy expenditure genes in BAT was not different between the two genotypes (Fig. 1C) (14). Moreover, SHP expression was not detected in C57BL/6 BAT (Fig. 1D), which is in accord with previous reports (21, 22).

We examined food intake and physical activity to understand the DIO resistance. $SHP^{-/-}$ mice exhibited comparable caloric intake to those of WT counterparts whether on CD or WestD (supplementary Fig. I). They also showed no significant statistical difference in physical activities, although $SHP^{-/-}$ mice exhibited a trend toward elevated locomotor activity in the 24 h measurement but a trend toward reduced vertical activity (Fig. 1E).

Increased oxygen consumption and respiratory quotient in $SHP^{-/-}$ mice

Indirect calorimetry was used to measure energy expenditure of the $SHP^{-/-}$ mice. Even though the function of BAT appeared normal compared with wild-type (WT) mice, $SHP^{-/-}$ mice consumed significantly more oxygen on either diet, especially during the dark cycle (**Fig. 2A**). Respiratory quotient (RQ), which measures substrate utilization, was higher in $SHP^{-/-}$ mice, suggesting higher carbohydrate utilization (Fig. 2B). The higher RQ may be accounted for by improved muscle insulin sensitivity of the null mice (see below). Elevated dietary fat decreases RQ in normal animals due to higher fat utilization (23). Although the RQ of WT mice fed WestD was decreased as expected, the RQ of $SHP^{-/-}$ mice fed WestD did not change compared with the CD-fed group, especially during the dark cycle (19:00–10:00) (supplementary Fig. II). This indicates that $SHP^{-/-}$ mice lack "metabolic flexibility" (23). However, the difference in the RQ between the two genotypes became minimal during fasting conditions (data not shown) or during the light cycle (11:00–18:00) in fed conditions.

Based on this differential energy utilization, we tested the physical endurance of $SHP^{-/-}$ mice. There was no difference in endurance between the two genotypes as shown by comparable running endurance on a treadmill (Fig. 2C). Interestingly, the measured VO_2max on a treadmill was still significantly higher in $SHP^{-/-}$ mice than in WT mice (Fig. 2D), suggesting that observed higher VO_2 in lean $SHP^{-/-}$ mice is from alterations in intrinsic metabolic pathways of energy utilization.

Elevated hepatic β-oxidation protects WestD-fed $SHP^{-/-}$ mice from hepatic steatosis

Consistent with earlier results, livers from WestD-fed WT mice were enlarged and pale, whereas $SHP^{-/-}$ livers were smaller and darker, resulting in a smaller liver to body weight ratio. Aged $SHP^{-/-}$ mice also showed smaller livers than age-matched WT mice (supplementary Fig. IIIA). This is due to differences in lipid accumulation, as shown in hematoxylin-eosin staining of the liver sections (supplementary Fig. IIIB) and hepatic TG and cholesterol levels (supplementary Fig. IIIC). We also observed moderately decreased serum lipid levels in $SHP^{-/-}$ mice (supplementary Fig. IIID).

To understand why $SHP^{-/-}$ mice accumulate less hepatic fat, we examined fatty acid oxidation and TG secretion.
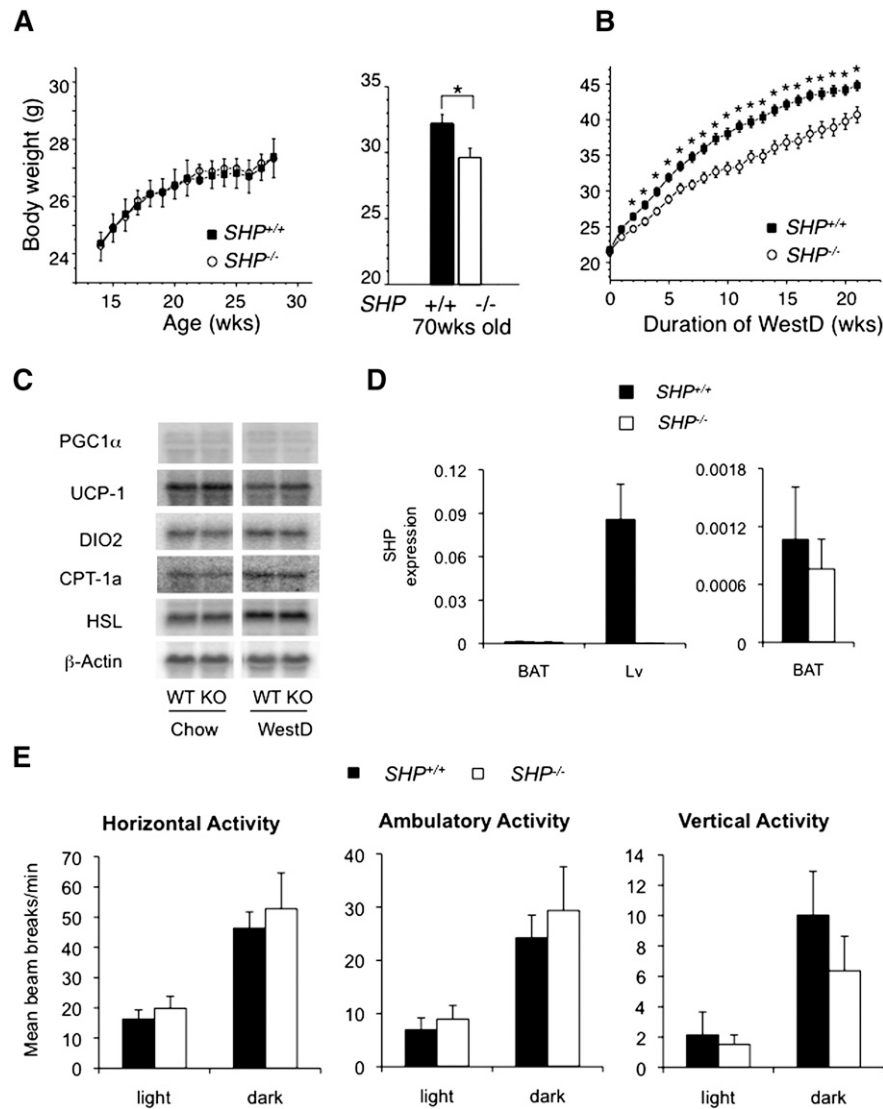
Fig. 1. Congenic $SHP^{-/-}$ mice werere protected from diet-induced obesity and maintained normal expression of genes responsible for energy expenditure in brown adipocytes. A: Growth curve of WT (n = 8) and $SHP^{-/-}$ mice (n = 8) fed standard rodent CD (4% fat; ≤0.04% cholesterol) (right panel) and body weights of WT (n = 4) and $SHP^{-/-}$ mice (n = 3) at 70 weeks of age fed CD (left panel). *, $P < 0.05$. B: Growth curve of 2-month-old WT and $SHP^{-/-}$ mice fed high-fat diet containing high fat and high cholesterol (21% milk fat, 0.2% cholesterol) for 22 weeks. Average of eight mice per each group was plotted with standard error. For statistics, Student's t-test was used at each time point. *, $P < 0.05$. C: Gene expression in BAT of WT and $SHP^{-/-}$ fed chow or WestD for 22 wks was determined by Northern blot analysis with indicated radiolabeled probes. D: qPCR amplification of SHP mRNA in BAT. SHP expression in BAT of WT and $SHP^{-/-}$ mice fed CD was compared with that in liver from the same animal (n = 4) (left panel). The expression in BAT from left panel was scaled up for comparison (right panel). E: Physical activity of the $SHP^{-/-}$ and WT mice fed chow. Three-month-old mice fed chow were used for 24 h (from noon on day 1 to noon on day 2) activity measurement. Average beam break numbers per minute from six mice were plotted with SEM.

The livers from $SHP^{-/-}$ mice exhibited significantly higher fatty acid oxidation than WT counterparts (**Fig. 3A**), resulting in higher plasma total ketone body level in the WestD-fed group (Fig. 3B). When hepatic TG secretion was measured for 20 h after injecting 1,000 mg/kg poloxamer 407, a strong inhibitor of lipoprotein lipase, we observed no difference between $SHP^{-/-}$ and WT mice (Fig. 3C). This result contrasts with the increased VLDL secretion previously described in $SHP^{-/-}$ mice relative to $SHP^{+/+}$ control mice either on ob/ob or C57BL/6 background (24). It should be noted, however, that the previous experiment used a different LPL inhibitor, tyloxapol, and monitored only the initial 2 h after injection of the LPL inhibitor.

SHP regulates the expression of genes involved in fatty acid oxidation upon WestD challenge

To determine the role of SHP in regulating fatty acid oxidation, we analyzed liver gene expression in WT and $SHP^{-/-}$ mice fed CD or WestD. Expression of major genes involved in fatty acid oxidation and ketone body formation was higher in $SHP^{-/-}$ mice fed WestD compared with their WT counterparts (**Fig. 4A**). The observed higher

TABLE 1. Analysis of body composition by PIXImus Densitometry

| | Chow | | WestD | |
	SHP^{+/+}	SHP^{−/−}	SHP^{+/+}	SHP^{−/−}
Number of mouse	6	4	4	4
Body Weight (g)	30.02 ± 1.49	27.8 ± 0.79	41 ± 0.91[a]	28.65 ± 0.7[b]
Lean Mass (g)	19.68 ± 0.79	18.73 ± 0.63	23.73 ± 0.49[a]	20.33 ± 0.38[b]
Fat (g)	4.43 ± 0.57	3.48 ± 0.31	10.68 ± 0.31[a]	3.73 ± 0.19[b]
% Fat	18.2 ± 1.88	15.6 ± 0.96	30.98 ± 0.71[a]	15.36 ± 0.73[b]
BMD (g/cm^2)	0.05 ± 0.0012	0.049 ± 0.0005	0.049 ± 0.0008	0.05 ± 0.0009
BMC (g)	0.47 ± 0.021	0.47 ± 0.025	0.39 ± 0.006[a]	0.49 ± 0.007[b]
Bone Area (cm^2)	9.45 ± 0.37	9.55 ± 0.46	7.87 ± 0.08[a]	10.03 ± 0.17[b]

Body compositions of WT and $SHP^{-/-}$ mice after 22 weeks WestD feeding presented as mean ± SEM. BMD, bone mineral density; BMC, bone mineral content. Data were obtained from a group of mice used in Fig. 2.
[a] $P < 0.009$ versus WT fed CD.
[b] $P < 0.002$ versus WT fed WestD.

mRNA expression appeared to be due to the lack of down-regulation response upon WestD challenge in $SHP^{-/-}$ animals. Expression of PPARα, a major transcription factor regulating β-oxidation, was not significantly different be-tween the two genotypes (Fig. 4C). In contrast, expression of major lipogenic genes was lower in $SHP^{-/-}$ mice fed WestD (Fig. 4B), consistent with decreased expression of SREBP1 and PPARγ (Fig. 4C). The observed decrease in
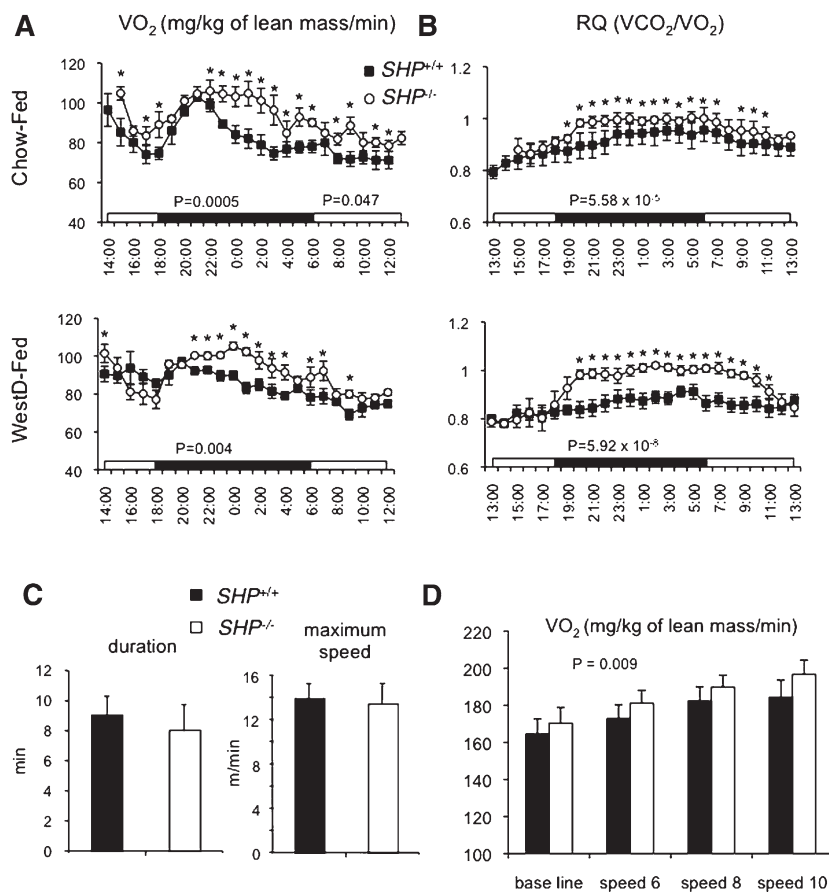

Fig. 2. Indirect calorimetry indicates that $SHP^{-/-}$ mice exhibit higher oxygen consumption (VO$_2$) and higher respiratory quotient. A, B: Mice fed chow diet (CD) (top panel) or WestD (center and bottom panel) were evaluated every 10 min for their VO$_2$ (A, normalized to lean mass) and RQ (B) in Oxymax chambers from Columbus Instruments while they were fed diets and water ad libitum. The average values for 1 h inter-val were plotted along with standard error. Student's t-test was used to compare genotypic significance at each time point. WT fed chow (n = 6), all other groups (n = 4), *, $P < 0.05$. C, D: The WestD-fed groups (n = 4) were placed in metabolic modular treadmills to measure their running endurance (C) and VO$_2$max (D). The starting treadmill speed was 6 m/min and speed and incline were raised every 2 min by 2 m/min and 5°, respectively. C: Average of their lasting time (left panel) and maximum speed (right panel) before fall-off were presented. D: Average VO$_2$ (normalized to lean mass) of 2 min measurement at each speed (m/min) was presented with SEM. P-value presents overall effect of genotype calculated by 2-way ANOVA.
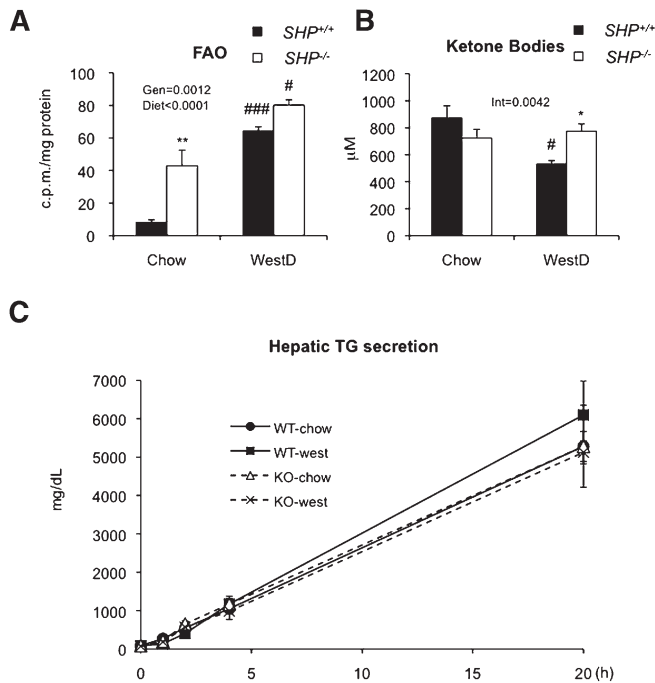
Fig. 3. Elevated fatty acid oxidation in $SHP^{-/-}$ liver. A: Fatty acid oxidation (FAO) of livers from WT and $SHP^{-/-}$ mice (n = 4/group) fed WestD for 12 weeks was assessed with [^{14}C] labeled palmitic acid as described in the Materials and Methods. Radioactivity in reaction buffer after assay was normalized to amount of the protein in the liver. B: Total ketone bodies from sera of WT and $SHP^{-/-}$ mice (n = 9 to 10) on 22wk-WestD regimen. C: Hepatic TG secretion from 4-month-old mice (n = 4) fed CD or WestD. Mice in WestD group were fed the diet for 3 weeks and injected i.p. 1,000 mg/kg poloxamer at 4 h after food removal. Serum TG levels were measured at 0, 1, 2, 4, and 20 h after the injection. A, B: Overall effect of genotype (Gen), diet, or their interaction (Int) were calculated by 2-way ANOVA. Bonferroni post hoc test results (* for genotype effect in the same diet group, # for diet effect of in the same genotypes) are as follows. *, #, $P < 0.05$; **, $P < 0.01$; ###, $P < 0.001$.

PPARγ expression is mostly due to the lack of PPARγ2 subtype (supplementary Fig. IV). The contribution of carbohydrate-response element-binding protein, a positive regulator of glycolysis and lipogenesis, to the liver phenotype of $SHP^{-/-}$ mice appeared minimal. Interestingly, the difference in the expression of some major genes was already noticeable after a 4 week WestD regimen (supplementary Fig. V). The higher β-oxidation rate in $SHP^{-/-}$ liver prompted us to test a regulatory role of SHP in PPARα-mediated transactivation. In a transient transfection assay, SHP selectively repressed RXR-ligand-activated PPARα transactivation of an Acox1 promoter driven luciferase reporter (Fig. 4E, top panel). The observed repression on the report gene activity is not mediated through possible RXR homodimer. Importantly, PPARα and SHP were corecruited to the Acox1 promoter in WT liver (Fig. 4E, bottom panel). These results suggest that SHP normally represses PPARα transactivation and target gene expression. Although the exact mechanism of how or when SHP is recruited to the PPARα target genes remains to be defined, we conclude that the loss of this repression contributes to the increased hepatic β-oxidation rate in $SHP^{-/-}$ livers fed WestD.

Altered mobilization of dietary fat is evident in $SHP^{-/-}$ mice

Surprisingly, lipid uptake genes were also significantly increased in $SHP^{-/-}$ mice (Fig. 4D). In order to examine hepatic lipid uptake directly, we treated mice by oral gavage with oil containing [^{14}C] labeled trioleoylglycerol and measured peripheral tissue radioactivity levels 4 h after challenge. As shown in Fig. 4F, significantly smaller amounts of labeled lipids were detected in white adipose tissue and muscle than in liver of $SHP^{-/-}$ mice compared with WT mice. Along with the gene expression result, this indicates that $SHP^{-/-}$ mice facilitate higher distribution of dietary lipids to liver than to other major peripheral tissues. Interestingly, overall tissue retention of the labeled lipids was smaller in $SHP^{-/-}$ mice, suggesting reduced intestinal fat absorption. Indeed, intestinal radioactivity levels remained higher in $SHP^{-/-}$ mice 4 h after oil challenge (supplementary Fig. VIB) and plasma radioactivity at 1 hr after the oil challenge was lower in $SHP^{-/-}$ mice (supplementary Fig. VIA).

$SHP^{-/-}$ mice exhibit severe glucose intolerance after WestD regimen

To assess glucose homeostasis in the $SHP^{-/-}$ mice, we performed a GTT after 22 weeks of the WestD regimen. The two genotypes fed CD showed no difference in GTT (supplementary Fig. VIIA). Surprisingly, the less obese $SHP^{-/-}$ mice on the WestD showed significantly impaired glucose clearance (**Fig. 5A**). Contrary to the glucose intolerance, $SHP^{-/-}$ mice had similar levels of baseline fasted serum glucose and insulin compared with WT mice whether fed CD or WestD (supplementary Fig. VIIB). Equally important, the ITT did not reveal differences in whole-body insulin sensitivity (Fig. 5B). Hepatic insulin sensitivity, assessed by levels of phosphorylated Akt upon insulin challenge, was decreased in the $SHP^{-/-}$ mice fed WestD (Fig. 5C), although it was not different when fed CD (supplementary Fig. VIII). On the contrary, $SHP^{-/-}$ skeletal muscle showed an opposite response. Thus, in $SHP^{-/-}$ mice, the compromised hepatic insulin sensitivity appeared to be compensated for by the muscle to maintain normal serum glucose despite apparent glucose intolerance in the animals. The observed muscle and hepatic insulin sensitivities can be supported by a relatively sharp decrease of serum glucose at later time point of the GTT (Fig. 5A) and by decreased glycogen storage and gene expression data showing increased gluconeogenesis and decreased glycolysis (**Fig. 6A**, C), respectively. Especially, higher gene expression of glucose-6-phosphatase and phosphoenolpyruvate carboxykinase, direct targets of HNF4α or PPARα transactivation (25–28), during WestD-feeding suggests a direct transcriptional regulatory role of SHP in the expression of these gluconeogenic genes (7). In addition, increased insulin sensitivity in the muscle resulted in decreased TG and glycogen contents associated with the observed lipid redistribution, enhanced glucose
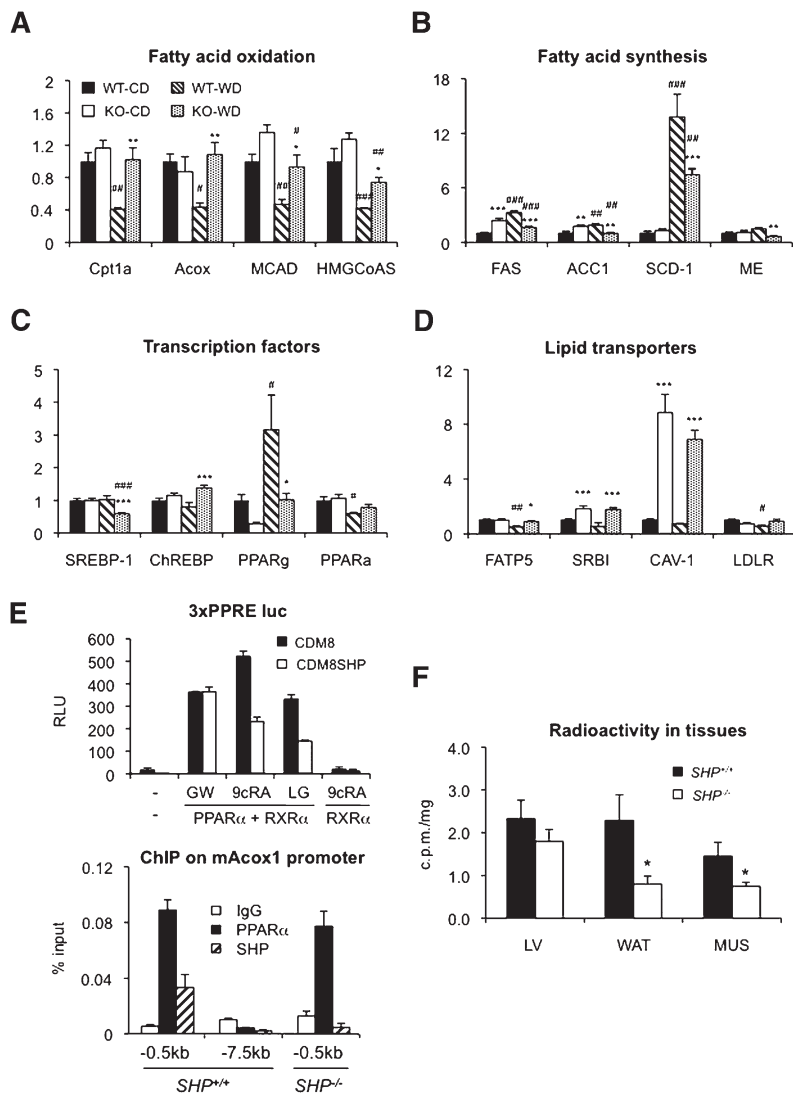
Fig. 4. Elevated expression of genes involved in fatty acid oxidation and uptake in $SHP^{-/-}$ mice fed WestD and association of PPARα signaling. RNAs isolated from livers of mice on the WestD regimen for 22 weeks were processed to quantify the expression of genes involved in fatty acid oxidation (A), fatty acid synthesis (B), responsible transcription factors (C), and lipid transporters (D) by quantitative real-time PCR. Average values of six mice per group except WT fed WestD (n = 5) were plotted with standard error. Significance of difference between genotype and diet were calculated by 2-way ANOVA with Bonferroni post hoc test results (* for genotype effect in the same diet group, # for diet effect of in the same genotypes). *, #, $P < 0.05$; **, $P < 0.01$; ###, $P < 0.001$. E: SHP represses PPARα mediated Acox1 expression. 3xPPRE luc reporter plasmid was cotransfected with PPARα and RXRα plasmids (50 ng each) into HepG2 cells. SHP repression on GW7647 (PPARα agonist, 2 nM), LG1069 (RXR agonist, 1 μM), or 9-cisRA (RXR agonist, 10 μM)-mediated PPARα transactivation was tested with cotransfection of CDM8 or CDM8mSHP (50 ng each) (top panel). ChIP assay was performed on the indicated Acox1 promoter regions in wild-type and $SHP^{-/-}$ mice liver. ChIP signals were analyzed using real-time qPCR and plotted as means ± SEM (bottom panel). F: Radioactivity levels in liver (LV), epididymal fat (WAT), and quadriceps (MUS) of 2.5-month-old mice fasted overnight at 4 h after oral challenge of radiolabeled TG (n = 5) were plotted with SEM. Student's t-test was used to calculate p-values between genotypes. *, $P < 0.05$.

utilization, and decreased expression of genes involved in fatty acid utilization (Fig. 6B, D).

The effects on insulin sensitivity in $SHP^{-/-}$ mice led us to explore islet function in GSIS. CD-fed $SHP^{-/-}$ mice showed no significant difference in insulin secretion compared with WT mice whereas WestD-fed $SHP^{-/-}$ mice had lower area under the curve than WT mice (28.9 ± 9.0 vs. 34.5 ± 10.1 min × ng/ml) (supplementary Fig. VIC). In order to gain clear insights into their islet function, we assessed GSIS with isolated islets from CD- and WestD-fed animals. GSIS at higher concentration of glucose was strongly compromised in islets from $SHP^{-/-}$ fed the WestD (Fig. 6E). In addition, insulin content in the isolated islets was also significantly reduced in $SHP^{-/-}$ mice.

DISCUSSION

The studies described here present a detailed and comprehensive analysis of the metabolic phenotypes of congenic C57BL/6 $SHP^{-/-}$ mice. These results show some general similarities with earlier results with mice on a mixed background, including resistance to both diet-in-

duced obesity and hepatic steatosis. Particularly in the case of overall energy balance and fat mobilization, however, the mechanisms are strikingly different. Thus, the congenic C57BL/6 $SHP^{-/-}$ mice did not exhibit BAT activation, but did show higher VO_2. In contrast to the majority of phenotypically lean mice (29–33), but in accord with some exceptions (34, 35), the $SHP^{-/-}$ mice showed elevated RQ, indicating increased carbohydrate oxidation. This increased whole-body RQ contrasts with the elevated fatty acid oxidation in the livers of the $SHP^{-/-}$ mice. Considering muscle as the major determinant for whole-body energy expenditure (36), we postulated that the higher RQ is a direct metabolic consequence of energy utilization as observed previously (34, 37, 38). This is consistent with the increased muscle insulin sensitivity as manifested by phospho-Akt levels and the decreased expression of genes involved in muscle fatty acid utilization such as *PGC-1α*, *Cpt1b*, and *FATP4* in $SHP^{-/-}$ mice. This may also explain their metabolic inflexibility, which is represented by high RQ values regardless of type of diets consumed.

The lack of lipid accumulation in the $SHP^{-/-}$ livers appears to be a direct effect of both decreased lipogenesis
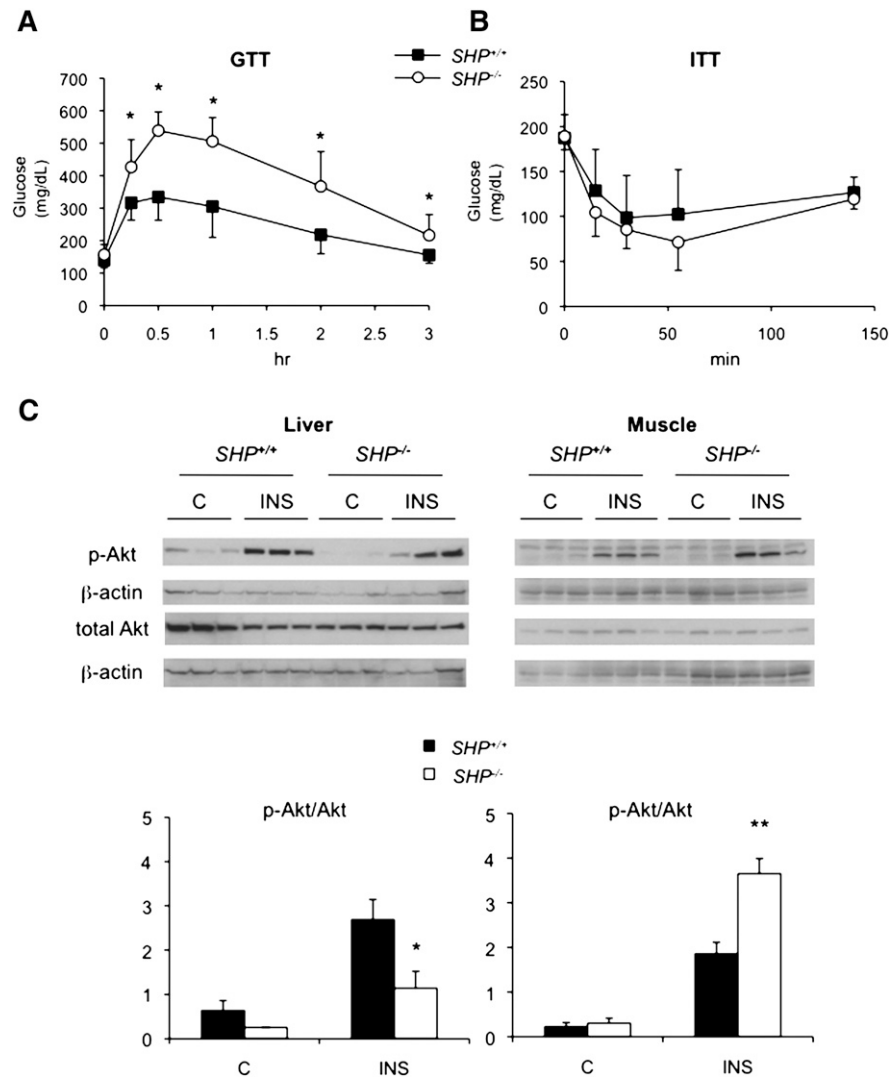
Fig. 5. WestD-fed $SHP^{-/-}$ mice exhibit severe whole body glucose intolerance with hepatic insulin resistance and muscle insulin sensitivity. A, B: GTT (A) and ITT (B) were performed with WT (n = 10 for GTT and n = 5 for ITT) and $SHP^{-/-}$ (n = 9 for GTT and n = 6 for ITT) mice fed WestD for 22 weeks by peritoneal injection of glucose (1 g/kg) and recombinant human insulin (1 U/kg), respectively. Values were presented as means ± SD. P-values were obtained using Student's *t*-test at each time point. *, $P < 0.015$. C: Liver and muscle insulin sensitivities were assessed by Western blot analysis evaluating the ratio of phosphoserine Akt to total Akt. Mice fed WestD were challenged intraperitoneally with 5 U/kg of human insulin for 5 min. Liver and muscle were collected and processed for Western blotting with the indicated antibodies. Specific protein bands were visualized by chemiluminescence (top panel). The specific Akt bands were quantified by densitometry analysis using Tina 2.0 software program and normalized to the corresponding β-actin bands. The results were presented as phospho-Akt to total Akt ratio (bottom panel). P-values were obtained from genotype comparison using Student's *t*-test. n = 3, *, $P = 0.003$; **, $P < 0.0001$.

and elevated fatty acid β-oxidation. The decreased expression of lipogenic genes is very consistent with the increase in hepatic lipogenesis in transgenic mice overexpressing SHP in the liver (39). Higher expression of fatty acid and cholesterol transporters such as *FATP5*, *SRBI*, and *LDLr* correlates with the increased lipid influx into the $SHP^{-/-}$ liver. The newly transported lipids are likely channeled to fatty acid oxidation directly as observed in muscle (40). The observed repression of fatty acid oxidation genes such as Acox1 and Mcad upon WestD feeding, which may contribute to the elevated incomplete

fatty acid oxidation (41), is consistent with other observations (42, 43). The enhanced fatty acid oxidation in WestD-fed but not chow-fed $SHP^{-/-}$ mice is associated with derepression of PPARα-mediated transactivation. This raises an interesting question of whether SHP itself senses nutritional status to repress β-oxidation only in the WestD-fed condition in the WT mice. This could reflect direct binding of nutritional metabolites to SHP, increased recruitment of SHP to the activated target nuclear receptors (especially RXR) by nutritional metabolites (44, 45), or increased SHP protein stability in WestD-fed mice (46).
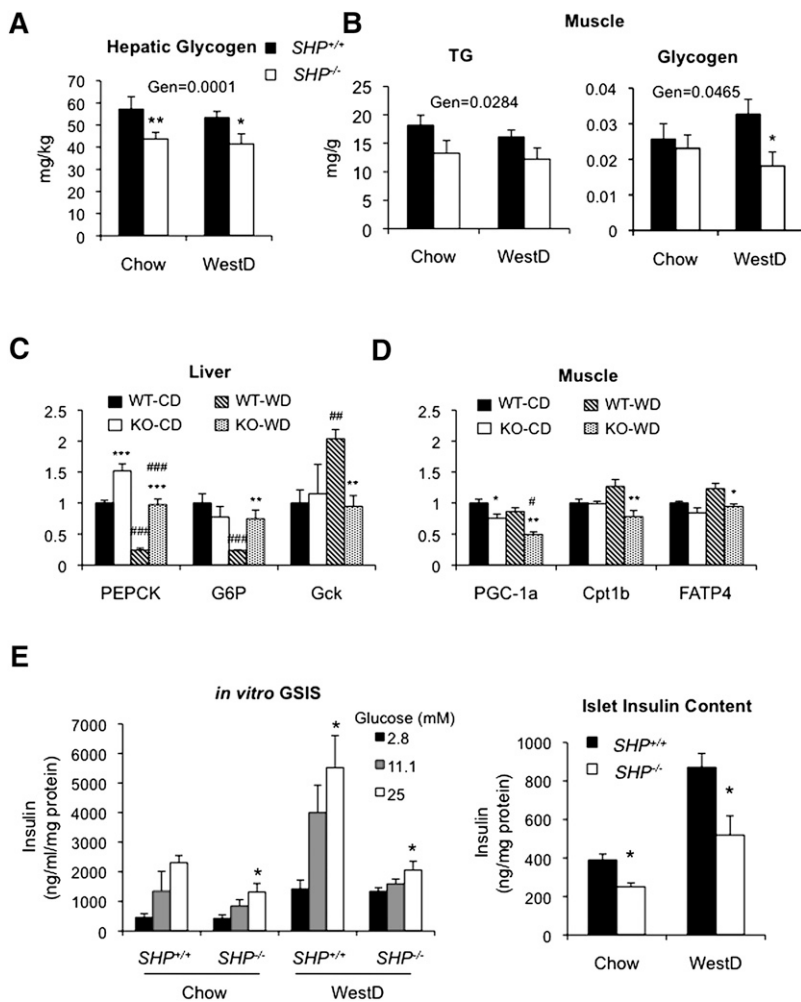
Fig. 6. Whole body glucose metabolism was assessed in $SHP^{-/-}$ mice. Livers were collected from WT and $SHP^{-/-}$ mice fed chow (CD) or WestD for 22 weeks and analyzed for glycogen content. The contents were normalized to liver weight and presented as means (n = 5) ± SEM. B: TG (left) and glycogen (right) contents in quadriceps from mice fed chow or WestD are presented as means (n = 7) ± SEM. Overall effects of genotype (Gen) were calculated by 2-way ANOVA. Bonferroni post hoc test results are as described in Figs. 3 and 4. C: RNAs from the livers were subjected to Northern analysis. Intensities of specific bands were quantified by a densitometry. Average values from three mice were presented along with SEM. PEPCK, phosphoenolpyruvate carboxykinase; G6P, glucose-6-phophatase; GcK, glucokinase. D: Expression of muscle genes were analyzed using qPCR and plotted as means (n = 5) ± SEM. 2-way ANOVA with Bonferroni posttest was used to calculate statistics. Boneferroni posttest results are as described previously. E: Glucose-stimulated insulin secretion in isolated islets from mice (n = 4) fed CD or WestD (22 weeks) in the presence of indicated amount of glucose (left panel). Their insulin content quantified by rat insulin ELISA after acid ethanol extraction (right panel). Student's *t* test results are presented. Left panel, versus 2.8 mM in the group; right panel, versus WT counterpart; *, $P < 0.05$.

The proposed redistribution of lipids to liver, which is more evident during WestD feeding, could alleviate diet-induced insulin resistance of peripheral tissues and aggravate hepatic insulin resistance, manifested by inducible phospho-Akt levels upon insulin challenge, which would be consistent with studies on $FATP5^{-/-}$, $FATP1^{-/-}$, or $CD36^{-/-}$ mice (47–51). In a manner analogous to paradigms of muscle insulin resistance, the relative increase in hepatic fatty acid delivery/oxidation could be associated with decreased glucose uptake/oxidation, thereby resulting in hepatic insulin resistance despite lowered TG accumulation (41, 50, 52). In particular, the insulin resistance of the $SHP^{-/-}$ liver is reminiscent of the unexpected insulin resistance of skeletal muscle in transgenic mice overexpressing PPARα, which was attributed to increased mitochondrial fatty acid β-oxidation (53). The redistribution of lipids to liver may also contribute to the overall lean phenotype, as observed with $FATP1^{-/-}$ mice, in which deficiency in muscle and adipose fatty acid uptake redirect dietary fat to liver (49). Additionally, reduced intestinal dietary fat absorption suggested by observations in Fig. 4F and supplementary Fig. VI could play a role in the observed lean phenotype of the diet induced model. However, this has a clear contrast to the increased bile acid secretion observed in $SHP^{-/-}$ mice (6). Moreover, fecal lipid contents were not significantly different between the two genotypes (data not shown). Thus, the altered dietary fat absorption should be further investigated to define its effect on the lean phenotype.

The $SHP^{-/-}$ mice did not show aberrant serum glucose or insulin level but did exhibit glucose intolerance upon glucose challenge after WestD regimen. This glucose intolerance could be explained by the islet dysfunction in GSIS, which is very consistent with the opposite results of a previous study with overexpression of SHP in rat islets (54). The anticipated lack of insulin secretion during the postprandial period may also contribute to the observed fasting-like hepatic phenotype in $SHP^{-/-}$ mice.

Overall, these results demonstrate that SHP regulates accumulation of excess dietary fat into liver. Loss of SHP function clearly protects the mice from development of obesity and hepatic steatosis, but with the cost of hepatic insulin resistance and islet dysfunction that makes the animals more susceptible to diet-induced diabetes.

REFERENCES

1. Lu, T. T., M. Makishima, J. J. Repa, K. Schoonjans, T. A. Kerr, J. Auwerx, and D. J. Mangelsdorf. 2000. Molecular basis for feedback regulation of bile acid synthesis by nuclear receptors. *Mol. Cell.* **6:** 507–515.

2. Goodwin, B., S. A. Jones, R. R. Price, M. A. Watson, D. D. McKee, L. B. Moore, C. Galardi, J. G. Wilson, M. C. Lewis, M. E. Roth, et al. 2000. A regulatory cascade of the nuclear receptors FXR, SHP-1, and LRH-1 represses bile acid biosynthesis. *Mol. Cell.* **6:** 517–526.

3. Kerr, T. A., S. Saeki, M. Schneider, K. Schaefer, S. Berdy, T. Redder, B. Shan, D. W. Russell, and M. Schwarz. 2002. Loss of nuclear receptor SHP impairs but does not eliminate negative feedback regulation of bile acid synthesis. *Dev. Cell.* **2:** 713–720.

4. Inagaki, T., M. Choi, A. Moschetta, L. Peng, C. L. Cummins, J. G. McDonald, G. Luo, S. A. Jones, B. Goodwin, J. A. Richardson, et al. 2005. Fibroblast growth factor 15 functions as an enterohepatic signal to regulate bile acid homeostasis. *Cell Metab.* **2:** 217–225.

5. Wang, L., Y-K. Lee, D. Bundman, Y. Han, S. Thevananther, C-S. Kim, S. S. Chua, P. Wei, R. A. Heyman, M. Karin, et al. 2002. Redundant pathways for negative feedback regulation of bile acid production. *Dev. Cell.* **2:** 721–731.

6. Park, Y. J., M. Qatanani, S. S. Chua, J. L. LaRey, S. A. Johnson, M. Watanabe, D. D. Moore, and Y. K. Lee. 2008. Loss of orphan receptor small heterodimer partner sensitizes mice to liver injury from obstructive cholestasis. *Hepatology.* **47:** 1578–1586.

7. Lee, Y. K., H. Dell, D. H. Dowhan, M. Hadzopoulou-Cladaras, and D. D. Moore. 2000. The orphan nuclear receptor SHP inhibits hepatocyte nuclear factor 4 and retinoid X receptor transactivation: two mechanisms for repression. *Mol. Cell. Biol.* **20:** 187–195.

8. Nishigori, H., H. Tomura, N. Tonooka, M. Kanamori, S. Yamada, K. Sho, I. Inoue, N. Kikuchi, K. Onigata, I. Kojima, et al. 2001. Mutations in the small heterodimer partner gene are associated with mild obesity in Japanese subjects. *Proc. Natl. Acad. Sci. USA.* **98:** 575–580.

9. Mitchell, S. M., M. N. Weedon, K. R. Owen, B. Shields, B. Wilkins-Wall, M. Walker, M. I. McCarthy, T. M. Frayling, and A. T. Hattersley. 2003. Genetic variation in the small heterodimer partner gene and young-onset type 2 diabetes, obesity, and birth weight in UK subjects. *Diabetes.* **52:** 1276–1279.

10. Hung, C. C., I. S. Farooqi, K. Ong, J. Luan, J. M. Keogh, M. Pembrey, G. S. Yeo, D. Dunger, N. J. Wareham, and S. O'Rahilly. 2003. Contribution of variants in the small heterodimer partner gene to birthweight, adiposity, and insulin levels: mutational analysis and association studies in multiple populations. *Diabetes.* **52:** 1288–1291.

11. Echwald, S. M., K. L. Andersen, T. I. Sorensen, L. H. Larsen, T. Andersen, N. Tonooka, H. Tomura, J. Takeda, and O. Pedersen. 2004. Mutation analysis of NR0B2 among 1545 Danish men identifies a novel c.278G>A (p.G93D) variant with reduced functional activity. *Hum. Mutat.* **24:** 381–387.

12. Bray, G. A., and T. Bellanger. 2006. Epidemiology, trends, and morbidities of obesity and the metabolic syndrome. *Endocrine.* **29:** 109–117.

13. Adams, L. A., J. F. Lymp, J. St Sauver, S. O. Sanderson, K. D. Lindor, A. Feldstein, and P. Angulo. 2005. The natural history of nonalcoholic fatty liver disease: a population-based cohort study. *Gastroenterology.* **129:** 113–121.

14. Wang, L., J. Liu, P. Saha, J. Huang, L. Chan, B. Spiegelman, and D. D. Moore. 2005. The orphan nuclear receptor SHP regulates PGC-1alpha expression and energy production in brown adipocytes. *Cell Metab.* **2:** 227–238.

15. Kliewer, S. A., K. Umesono, D. J. Noonan, R. A. Heyman, and R. M. Evans. 1992. Convergence of 9-cis retinoic acid and peroxisome proliferator signalling pathways through heterodimer formation of their receptors. *Nature.* **358:** 771–774.

16. Lee, Y. K., Y. H. Choi, S. Chua, Y. J. Park, and D. D. Moore. 2006. Phosphorylation of the hinge domain of the nuclear hormone receptor LRH-1 stimulates transactivation. *J. Biol. Chem.* **281:** 7850–7855.

17. Seed, B. 1987. An LFA-3 cDNA encodes a phospholipid linked membrane protein homologous to its receptor, CD2. *Nature.* **329:** 840–842.

18. Mao, J., F. J. DeMayo, H. Li, L. Abu-Elheiga, Z. Gu, T. E. Shaikenov, P. Kordari, S. S. Chirala, W. C. Heird, and S. J. Wakil. 2006. Liver-specific deletion of acetyl-CoA carboxylase 1 reduces hepatic triglyceride accumulation without affecting glucose homeostasis. *Proc. Natl. Acad. Sci. USA.* **103:** 8552–8557.

19. Kim, J. Y., T. R. Koves, G. S. Yu, T. Gulick, R. N. Cortright, G. L. Dohm, and D. M. Muoio. 2002. Evidence of a malonyl-CoA-insensitive carnitine palmitoyltransferase I activity in red skeletal muscle. *Am. J. Physiol. Endocrinol. Metab.* **282:** E1014–E1022.

20. Millar, J. S., D. A. Cromley, M. G. McCoy, D. J. Rader, and J. T. Billheimer. 2005. Determining hepatic triglyceride production in mice: comparison of poloxamer 407 with Triton WR-1339. *J. Lipid Res.* **46:** 2023–2028.

21. Bookout, A. L., Y. Jeong, M. Downes, R. T. Yu, R. M. Evans, and D. J. Mangelsdorf. 2006. Anatomical profiling of nuclear receptor expression reveals a hierarchical transcriptional network. *Cell.* **126:** 789–799.

22. Yang, X., M. Downes, R. T. Yu, A. L. Bookout, W. He, M. Straume, D. J. Mangelsdorf, and R. M. Evans. 2006. Nuclear receptor expression links the circadian clock to metabolism. *Cell.* **126:** 801–810.

23. Galgani, J. E., C. Moro, and E. Ravussin. 2008. Metabolic flexibility and insulin resistance. *Am. J. Physiol. Endocrinol. Metab.* **295:** E1009–E1017.

24. Huang, J., J. Iqbal, P. K. Saha, J. Liu, L. Chan, M. M. Hussain, D. D. Moore, and L. Wang. 2007. Molecular characterization of the role of orphan receptor small heterodimer partner in development of fatty liver. *Hepatology.* **46:** 147–157.

25. Rajas, F., A. Gautier, I. Bady, S. Montano, and G. Mithieux. 2002. Polyunsaturated fatty acyl coenzyme A suppress the glucose-6-phosphatase promoter activity by modulating the DNA binding of hepatocyte nuclear factor 4 alpha. *J. Biol. Chem.* **277:** 15736–15744.

26. Yoon, J. C., P. Puigserver, G. Chen, J. Donovan, Z. Wu, J. Rhee, G. Adelmant, J. Stafford, C. R. Kahn, D. K. Granner, et al. 2001. Control of hepatic gluconeogenesis through the transcriptional coactivator PGC-1. *Nature.* **413:** 131–138.

27. Scribner, K. B., D. P. Odom, and M. M. McGrane. 2007. Nuclear receptor binding to the retinoic acid response elements of the phosphoenolpyruvate carboxykinase gene in vivo: effects of vitamin A deficiency. *J. Nutr. Biochem.* **18:** 206–214.

28. Im, S. S., M. Y. Kim, S. K. Kwon, T. H. Kim, J. S. Bae, H. Kim, K. S. Kim, G. T. Oh, and Y. H. Ahn. 2011. Peroxisome proliferator-activated receptor {alpha} is responsible for the up-regulation of hepatic glucose-6-phosphatase gene expression in fasting and db/db mice. *J. Biol. Chem.* **286:** 1157–1164.

29. Zhou, Z., S. Yon Toh, Z. Chen, K. Guo, C. P. Ng, S. Ponniah, S. C. Lin, W. Hong, and P. Li. 2003. Cidea-deficient mice have lean phenotype and are resistant to obesity. *Nat. Genet.* **35:** 49–56.

30. Martin, T. L., T. Alquier, K. Asakura, N. Furukawa, F. Preitner, and B. B. Kahn. 2006. Diet-induced obesity alters AMP kinase activity in hypothalamus and skeletal muscle. *J. Biol. Chem.* **281:** 18933–18941.

31. Chadt, A., K. Leicht, A. Deshmukh, L. Q. Jiang, S. Scherneck, U. Bernhardt, T. Dreja, H. Vogel, K. Schmolz, R. Kluge, et al. 2008. Tbc1d1 mutation in lean mouse strain confers leanness and protects from diet-induced obesity. *Nat. Genet.* **40:** 1354–1359.

32. Pelletier, P., K. Gauthier, O. Sideleva, J. Samarut, and J. E. Silva. 2008. Mice lacking the thyroid hormone receptor-alpha gene spend more energy in thermogenesis, burn more fat, and are less sensitive to high-fat diet-induced obesity. *Endocrinology.* **149:** 6471–6486.

33. Liu, X., M. Rossmeisl, J. McClaine, M. Riachi, M. E. Harper, and L. P. Kozak. 2003. Paradoxical resistance to diet-induced obesity in UCP1-deficient mice. *J. Clin. Invest.* **111:** 399–407.

34. Newberry, E. P., Y. Xie, S. M. Kennedy, J. Luo, and N. O. Davidson. 2006. Protection against Western diet-induced obesity and hepatic steatosis in liver fatty acid-binding protein knockout mice. *Hepatology.* **44:** 1191–1205.

35. Katic, M., A. R. Kennedy, I. Leykin, A. Norris, A. McGettrick, S. Gesta, S. J. Russell, M. Bluher, E. Maratos-Flier, and C. R. Kahn. 2007. Mitochondrial gene expression and increased oxidative metabolism: role in increased lifespan of fat-specific insulin receptor knock-out mice. *Aging Cell.* **6:** 827–839.

36. Zurlo, F., K. Larson, C. Bogardus, and E. Ravussin. 1990. Skeletal muscle metabolism is a major determinant of resting energy expenditure. *J. Clin. Invest.* **86:** 1423–1427.

37. Turner, N., C. R. Bruce, S. M. Beale, K. L. Hoehn, M. So, M. S. Rolph, and G. J. Cooney. 2007. Excess lipid availability increases mitochondrial fatty acid oxidative capacity in muscle: evidence against a role for reduced fatty acid oxidation in lipid-induced insulin resistance in rodents. *Diabetes.* **56:** 2085–2092.

38. Haramizu, S., A. Nagasawa, N. Ota, T. Hase, I. Tokimitsu, and T. Murase. 2009. Different contribution of muscle and liver lipid metabolism to endurance capacity and obesity susceptibility of mice. *J. Appl. Physiol.* **106:** 871–879.

39. Boulias, K., N. Katrakili, K. Bamberg, P. Underhill, A. Greenfield, and I. Talianidis. 2005. Regulation of hepatic metabolic pathways by the orphan nuclear receptor SHP. *EMBO J.* **24:** 2624–2633.

40. Nickerson, J. G., H. Alkhateeb, C. R. Benton, J. Lally, J. Nickerson, X. X. Han, M. H. Wilson, S. S. Jain, L. A. Snook, J. F. Glatz, et al. 2009. Greater transport efficiencies of the membrane fatty acid transporters FAT/CD36 and FATP4 compared with FABPpm and FATP1 and differential effects on fatty acid esterification and oxidation in rat skeletal muscle. *J. Biol. Chem.* **284:** 16522–16530.

41. Koves, T. R., J. R. Ussher, R. C. Noland, D. Slentz, M. Mosedale, O. Ilkayeva, J. Bain, R. Stevens, J. R. Dyck, C. B. Newgard, et al. 2008. Mitochondrial overload and incomplete fatty acid oxidation contribute to skeletal muscle insulin resistance. *Cell Metab.* **7:** 45–56.

42. Badman, M. K., P. Pissios, A. R. Kennedy, G. Koukos, J. S. Flier, and E. Maratos-Flier. 2007. Hepatic fibroblast growth factor 21 is regulated by PPARalpha and is a key mediator of hepatic lipid metabolism in ketotic states. *Cell Metab.* **5:** 426–437.

43. Leavens, K. F., R. M. Easton, G. I. Shulman, S. F. Previs, and M. J. Birnbaum. 2009. Akt2 is required for hepatic lipid accumulation in models of insulin resistance. *Cell Metab.* **10:** 405–418.

44. Keller, H., C. Dreyer, J. Medin, A. Mahfoudi, K. Ozato, and W. Wahli. 1993. Fatty acids and retinoids control lipid metabolism through activation of peroxisome proliferator-activated receptor-retinoid X receptor heterodimers. *Proc. Natl. Acad. Sci. USA.* **90:** 2160–2164.

45. Yuan, X., T. C. Ta, M. Lin, J. R. Evans, Y. Dong, E. Bolotin, M. A. Sherman, B. M. Forman, and F. M. Sladek. 2009. Identification of an endogenous ligand bound to a native orphan nuclear receptor. *PLoS ONE.* **4:** e5609.

46. Miao, J., Z. Xiao, D. Kanamaluru, G. Min, P. M. Yau, T. D. Veenstra, E. Ellis, S. Strom, K. Suino-Powell, H. E. Xu, et al. 2009. Bile acid signaling pathways increase stability of small heterodimer partner (SHP) by inhibiting ubiquitin-proteasomal degradation. *Genes Dev.* **23:** 986–996.

47. Goudriaan, J. R., V. E. Dahlmans, B. Teusink, D. M. Ouwens, M. Febbraio, J. A. Maassen, J. A. Romijn, L. M. Havekes, and P. J. Voshol. 2003. CD36 deficiency increases insulin sensitivity in muscle, but induces insulin resistance in the liver in mice. *J. Lipid Res.* **44:** 2270–2277.

48. Hajri, T., X. X. Han, A. Bonen, and N. A. Abumrad. 2002. Defective fatty acid uptake modulates insulin responsiveness and metabolic responses to diet in CD36-null mice. *J. Clin. Invest.* **109:** 1381–1389.

49. Wu, Q., A. M. Ortegon, B. Tsang, H. Doege, K. R. Feingold, and A. Stahl. 2006. FATP1 is an insulin-sensitive fatty acid transporter involved in diet-induced obesity. *Mol. Cell. Biol.* **26:** 3455–3467.

50. Kim, J. K., R. E. Gimeno, T. Higashimori, H. J. Kim, H. Choi, S. Punreddy, R. L. Mozell, G. Tan, A. Stricker-Krongrad, D. J. Hirsch, et al. 2004. Inactivation of fatty acid transport protein 1 prevents fat-induced insulin resistance in skeletal muscle. *J. Clin. Invest.* **113:** 756–763.

51. Doege, H., R. A. Baillie, A. M. Ortegon, B. Tsang, Q. Wu, S. Punreddy, D. Hirsch, N. Watson, R. E. Gimeno, and A. Stahl. 2006. Targeted deletion of FATP5 reveals multiple functions in liver metabolism: alterations in hepatic lipid homeostasis. *Gastroenterology.* **130:** 1245–1258.

52. Choi, C. S., D. E. Befroy, R. Codella, S. Kim, R. M. Reznick, Y. J. Hwang, Z. X. Liu, H. Y. Lee, A. Distefano, V. T. Samuel, et al. 2008. Paradoxical effects of increased expression of PGC-1alpha on muscle mitochondrial function and insulin-stimulated muscle glucose metabolism. *Proc. Natl. Acad. Sci. USA.* **105:** 19926–19931.

53. Finck, B. N., C. Bernal-Mizrachi, D. H. Han, T. Coleman, N. Sambandam, L. l. LaRiviere, J. O. Holloszy, C. F. Semenkovich, and D. P. Kelly. 2005. A potential link between muscle peroxisome proliferator-activated receptor-α signaling and obesity-related diabetes. *Cell Metab.* **1:** 133–144.

54. Suh, Y. H., S. Y. Kim, H. Y. Lee, B. C. Jang, J. H. Bae, J. N. Sohn, S. I. Suh, J. W. Park, K. U. Lee, and D. K. Song. 2004. Overexpression of short heterodimer partner recovers impaired glucose-stimulated insulin secretion of pancreatic beta-cells overexpressing UCP2. *J. Endocrinol.* **183:** 133–144.